Hindrance of complete fusion in the ^{8}Li + ^{208}Pb system at above-barrier energies

E. F. Aguilera,* E. Martinez-Quiroz, and P. Rosales
Departamento de Aceleradores, ININ, A. P. 18-1027, C. P. 11801, México, D.F., México

J. J. Kolata
Physics Department, University of Notre Dame, Notre Dame, Indiana, 46556-5670, USA

P. A. DeYoung, G. F. Peaslee, P. Mears, and C. Guess
Physics Department, Hope College, Holland, Michigan, 49422-9000, USA

F. D. Becchetti, J. H. Lupton, and Yu Chen
Physics Department, University of Michigan, Ann Arbor, Michigan, 48109-1120, USA
(Received 13 April 2009; published 9 October 2009)

The ^{211,212}At yields resulting from the interaction of the radioactive projectile ^{8}Li with a ^{208}Pb target have been measured at energies between 3 and 8.5 MeV above the Coulomb barrier. They are signatures for fusion of the whole charge but not necessarily the whole mass of the projectile, so they are included in a corresponding operational definition of complete fusion. Within this definition, a fusion suppression factor of 0.70 ± 0.02 (stat.) ± 0.04 (syst.) is deduced from a comparison to a one-dimensional barrier-penetration-model calculation using parameters extrapolated from values for ^{6,7}Li + ^{209}Bi and ^{9}Be + ^{208}Pb taken from the literature. Possible incomplete fusion processes are discussed and the results are fitted with a phenomenological model assuming breakup prior to fusion followed by capture of a ^{7}Li fragment.

DOI: 10.1103/PhysRevC.80.044605 PACS number(s): 25.60.Pj, 25.70.−z

I. INTRODUCTION

Lately much work has been done with weakly bound light nuclei, both stable and short-lived, i.e., radioactive. The ^{6}He + ^{209}Bi system, for instance, has been found to present extremely interesting features. Because of the weakly bound neutron-halo nature of the ^{6}He projectile, the direct transfer/breakup processes dominate in the energy region below the barrier [1,2], leading to enhanced reaction cross sections. In fact, this feature seems to be a general signature of systems with neutron-halo nuclei [3]. Similarly, the proton-halo system ^{8}B + ^{58}Ni also recently was shown to display enhanced reaction cross sections below the barrier [4], but in this case the process is most probably driven by projectile breakup. Direct reactions also have been observed to be quite important near the barrier for stable but weakly bound projectiles [5]. The above scenario contrasts with observations for more normal, tightly bound nuclei for which fusion nearly exhausts the total reaction cross section at sub-barrier energies [6,7].

Breakup seems to dominate in the vicinity of the Coulomb barrier for many systems having loosely bound projectiles (though not the neutron-halo systems as mentioned above). The complete fusion (CF) cross sections, where the target absorbs the entire projectile, have been observed for some systems to present an above-barrier suppression with respect to bare (no-coupling) one-dimensional barrier-penetration-model (BPM) calculations, possibly due to breakup effects. Another possible effect of breakup on fusion (in addition to reduction of the fusion yield) might be the occurrence of "incomplete fusion" (ICF) [5], i.e., the absorption of a portion of the projectile.

For neutron-halo systems, the most important component of direct reactions seems to be neutron transfer channels with only a small contribution from breakup. This has been shown experimentally, e.g., for ^{6}He + ^{209}Bi [8–10] and ^{6}He + ^{65}Cu [11], and substantiated by calculations for other systems [3]. Neutron-transfer couplings also can produce a fusion hindrance above the barrier [12]. In fact, Keeley *et al.* [3] concluded that the total fusion (TF) of neutron-halo systems consistently shows an above-barrier suppression with respect to BPM calculations. This has been confirmed in the more recent analysis of Canto *et al.* [13], who, in addition, argue that for these systems TF $\sim$ CF, so the same conclusion should hold for CF.

Distinguishing between ICF and CF is quite challenging from both the experimental and the theoretical point of view (for recent reviews see Refs. [3,5]). A few experiments have been performed where a separation of CF from ICF was achieved for some systems with weakly bound stable projectiles, among them ^{9}Be + ^{208}Pb and ^{6,7}Li + ^{209}Bi [14–16]. Because experimental barrier distributions also were derived for these systems, a reliable comparison with BPM calculations could be made and a CF suppression close to 30% was observed above the barrier. The individual suppression factors were correlated with the breakup threshold energy (S_{bu}) of the projectile. The lower the value of S_{bu}, the larger the CF suppression. Similar correlations have been observed for other projectile-target combinations such as ^{7}Li + ^{165}Ho [17], ^{6}Li + ^{208}Pb [18], (^{11}B, ^{10}B, ^{7}Li) + ^{159}Tb [19], and (^{11}B, ^{10}B) + ^{209}Bi [20]. (The CF suppression seems to be considerably smaller for ^{9}Be + ^{144}Sm [21] and quite

*eli.aguilera@inin.gob.mx

small for even lighter targets [5]). In spite of extensive work [14–16,18,22–33], there is not yet a definitive explanation of the influence of breakup on fusion. Thus it is important to study additional systems where transfer/breakup processes are likely to occur near the barrier.

The short-lived radioactive nucleus ^{8}Li is an interesting subject to study within this context. It is weakly bound, with a threshold breakup energy $S_{^{7}\mathrm{Li}+n} = 2.033$ MeV, which lies between those for ^{6}Li ($S_{\alpha+d} = 1.475$ MeV) and ^{7}Li ($S_{\alpha+t} = 2.468$ MeV). Large transfer/breakup yields (up to nearly 300 mb) have been reported for $^{8}\mathrm{Li} + ^{208}\mathrm{Pb}$ [34] at energies near and below the Coulomb barrier. A very detailed search for a threshold anomaly in this system provides evidence that none is present [35]. A DWBA and CCBA analysis of the elastic and one-neutron removal channels, which includes transfer and breakup processes, predicts that the observed ^{7}Li yield is produced mainly by $1n$ transfer, with only a small contribution from breakup [36,37]. In this respect, this is similar to the situation for neutron-halo nuclei. However, an additional α-particle yield was observed [34], possibly resulting from subsequent breakup of the ^{7}Li [38]. CF supression may then be expected for this system above the barrier, and one might wonder if it will show the "normal" suppression factors observed for nonhalo weaklybound projectiles or display an increased suppression resulting from the combined effect of the known transfer and breakup channels. Within this context, and with the purpose of further investigating reaction mechanisms in the $^{8}\mathrm{Li} + ^{208}\mathrm{Pb}$ system, CF measurements at energies a few MeV above the Coulomb barrier are reported here. Preliminary results have been presented earlier in Ref. [39].

II. EXPERIMENTAL PROCEDURE

The ^{8}Li beam was generated by means of the one-neutron-transfer reaction $^{9}\mathrm{Be}(^{7}\mathrm{Li}, ^{8}\mathrm{Li})^{8}\mathrm{Be}$, using the TwinSol radioactive nuclear beam facility at the University of Notre Dame (UND) ([34] and Refs. therein). The UND FN tandem accelerator was used to deliver primary $^{7}\mathrm{Li}^{3+}$ beams with energies between 36 and 42 MeV in 1-MeV steps. These produced ^{8}Li beams with center-of-mass energies (at the target center) of 32.1, 33.0, 33.9, 34.8, 35.7, 36.6, and 37.5 MeV, respectively. The typical primary beam current was 170 particle nA, yielding secondary beam rates of 2×10^{5} particles/s. The corresponding energy width was approximately 1 MeV full width at half maximum (FWHM). The secondary beam from TwinSol is generally contaminated by unwanted ions having the same magnetic rigidity. In the present case the main contaminants and respective typical yields (relative to ^{8}Li) were $^{4}\mathrm{He}^{2+}$(40%) and $^{7}\mathrm{Li}^{2+}$(20%). The lower mass of the primary beam and the positive Q value for ^{8}Li prevented a $^{7}\mathrm{Li}^{3+}$ contamination. The $^{7}\mathrm{Li}^{2+}$ component was not a concern because the corresponding energy was always considerably below the respective Coulomb barrier. However, the ^{4}He beam component was of some concern, as discussed below. The target was a 1.8 mg/cm^{2} foil of isotopically separated ^{208}Pb having an isotopic purity better than 99%.

After $4n$ emission from the compound nucleus ^{216}At, the excited ^{212}At evaporation residue can be produced in its 1^{-} ground state, which decays with a half-life of 314 ms by the emission of two closely spaced α-particle groups with an average energy $E(\alpha_1) = 7662$ keV. Alternatively, the 9^{-} isomeric state could be populated. This state has a half-life of 119 ms and again decays via the emission of two closely spaced α-particle groups, in this case having an average energy $E(\alpha_2) = 7848$ keV. The $5n$ evaporation channel eventually populates the $9/2^{-}$ ground state of ^{211}At, which has a half-life of 7.2 h and decays 42% of the time by emission of an α particle of $E(\alpha_3) = 5870$ keV. The remaining 58% of the time, ^{211}At decays by electron capture (EC) to ^{211}Po, which quickly emits a 7450 keV α particle (α_4).

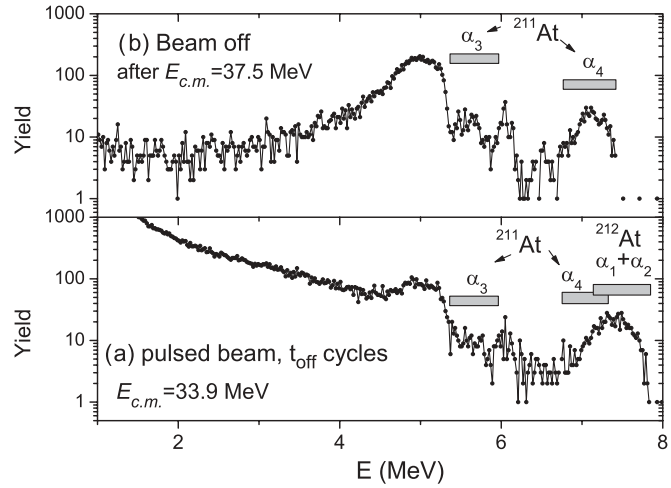

FIG. 1. Typical spectra obtained at the "box" detector. (a) The delayed activity measured for all beam-off cycles of the pulsed beam was summed. The energy regions of the α-particle groups of interest (see text) are indicated with rectangles. The bump at the left of the α_3 group probably corresponds to ^{209,210}Po activity produced by the ^{4}He contaminant beam. (b) Spectrum obtained with the beam completely off, taken immediately after bombardement with ^{8}Li ions having $E_{\mathrm{c.m.}} = 37.5$ MeV. The positions of the "long-life" α particles ($T_{1/2} = 7.2$ h) produced in the decay of ^{211}At are indicated.

The delayed α particles were detected in a "box" consisting of four large-area (3 cm × 3 cm) Si detectors placed in front of the target, i.e., in the backward hemisphere. This "box" was used in a previous work [40], where a coverage efficiency of $21 \pm 1\%$ was determined. Two 600 mm^{2} Si detectors placed at $\pm 45^{\circ}$ served as beam monitors for normalization purposes. A schematic diagram of the detector array can be found in Ref. [39].

To eliminate the background coming from prompt reactions, the primary beam was pulsed with a 0.6 s (0.7 s) "beam-on" ("beam-off") period, and the time of each event relative to the begining of a counting cycle was recorded. Figure 1(a) shows a typical spectrum obtained by counting the activity during the "beam-off" cycles.

The ^{4}He contaminant beam may produce undesired α activity through the fusion-evaporation process, i.e., 5.3 MeV α's from ^{210}Po ($T_{1/2} = 138$ d), corresponding to $2n$ emission, and 4.9 MeV α's from ^{209}Po ($T_{1/2} = 102$ y), resulting from $3n$ evaporation. The bump centered at about 5 MeV is most probably originated in this process. This bump prevented

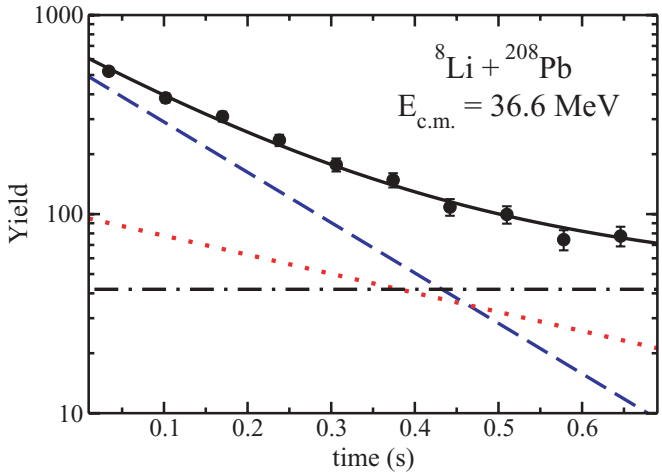

FIG. 2. (Color online) Typical time-decay curve for the α-particle groups with energies between 7.45 and 7.85 MeV. The dashed and dotted lines correspond to half-lives of 119 and 314 ms, respectively, while the dash-dotted line is the background produced by the "slow-decay" α' particles ($T_{1/2} = 7.2$ h). The solid line is the sum of all three decay curves.

a clean separation of the α_3 group, which could not be resolved (see Fig. 1). The energy resolution of the detectors was insufficient to resolve the closely spaced groups whose energies differ only by the 63.5-keV excitation energy of the 4^+ state in ^{208}Bi. Separation of the ground state from the isomeric-state decay in ^{212}At, or from the 7450-keV α particles from ^{211}Po, was not possible using α-particle energy measurements. Identification was, however, achieved from the difference in decay curves (Fig. 2).

A beam-leakage fraction was determined for each experimental run from the monitor counts during the beam-off period. Except for the lowest energy run, where the leaked beam was about 5% of the T$_{on}$ beam, this fraction was quite small, averaging to 1% for all seven runs. The corresponding contribution was taken into account by subtracting the respective background from the delayed α-particle group. Figure 2 shows a typical decay curve, illustrating the unfolding of the three decay processes that could be achieved. Note that the "slow-decay" 7450-keV α particles produce a flat background in this curve that must be subtracted to determine the yield of the $4n$ channel.

As for the yield of the $5n$ channel, long runs (several hours) of "beam-off" counting were made after the 36.6- and 37.5-MeV bombardments. The spectrum obtained for the last case is shown in Fig. 1(b). At these energies, calculations using the code PACE2 [41] indicated important contributions from $5n$ evaporation. The two experimental points thus obtained were used to determine the flat background in the corresponding time-decay curves of the "rapid decay" α-particle groups (see Fig. 2, which shows the data taken at 36.6 MeV). These two points were also used to extrapolate, with the help of PACE2 calculations, to the region of lower energies to estimate the corresponding flat-background contributions for those points where the $5n$ channel was not measured.

TABLE I. Cross sections for the ^{211,212}At evaporation residues. Column 4 is the calculated yield[a] for other evaporation channels and the last column gives the adopted "CF" cross sections (see text).

$E_{c.m.}$ (MeV)	σ(^{212}At) (mb)	σ(^{211}At) (mb)	σ(others) (mb)	σ("CF") (mb)
32.1	211 ± 7	0.1 ± 0.06[b]	41.4 ± 3.6	251 ± 9
33.0	276 ± 8	1.0 ± 0.2[b]	32.7 ± 3.9	309 ± 9
33.9	383 ± 12	7.2 ± 0.9[b]	27.5 ± 3.3	403 ± 13
34.8	393 ± 10	33.5 ± 4.4[b]	20.7 ± 2.2	450 ± 12
35.7	426 ± 10	92.2 ± 8.7[b]	18.2 ± 1.8	526 ± 13
36.6	418 ± 10	162.0 ± 8.5	16.1 ± 1.5	590 ± 13
37.5	370 ± 11	253.9 ± 6.6	14.8 ± 0.9	638 ± 13

[a]Uncertainties in calculated values are explained in the text.
[b]Extrapolated (see Fig. 5).

III. EXPERIMENTAL RESULTS

The fusion cross sections obtained for the ^{211,212}At evaporation residues are reported in Table I and shown in Fig. 3. The error bars include effects of counting statistics, detector efficiency, and leaked-beam determination. It is worth mentioning that two different groups did independent analyses of the data using different techniques [42] and arrived at essentially the same results. A systematic error of ±2.8% is estimated from the difference between the results of these two independent analyses. Also shown in Fig. 3 are the results of a PACE2 evaporation calculation for the $4n$ and $5n$ channels. Only default parameters were used in all our PACE2 calculations except that we did not use the Bass-barrier parameters [43] in the entrance channel. Instead, the barrier parameters used in the present work were extrapolated from those for neighboring systems (^{6,7}Li + ^{209}Bi and ^{9}Be + ^{208}Pb) for which the corresponding barrier distributions have been

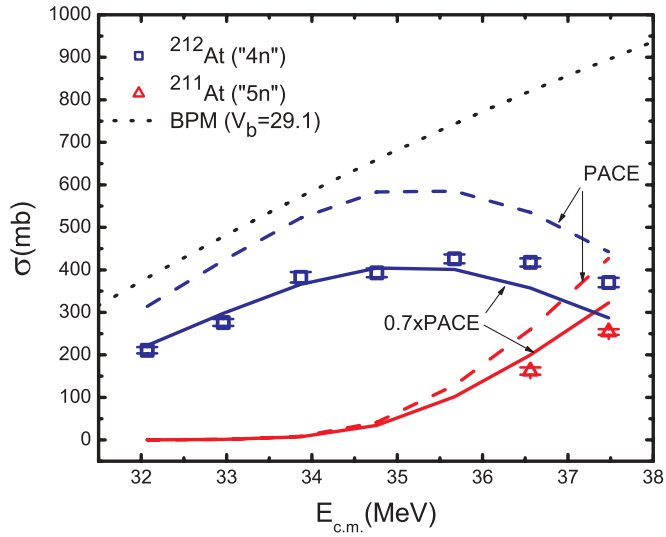

FIG. 3. (Color online) Experimental excitation functions for the ^{211,212}At fusion-evaporation residues in the ^{8}Li + ^{208}Pb system. PACE2 predictions are also shown. The BPM curve represents the input cross sections used in PACE2. See text for a complete description of the different curves.

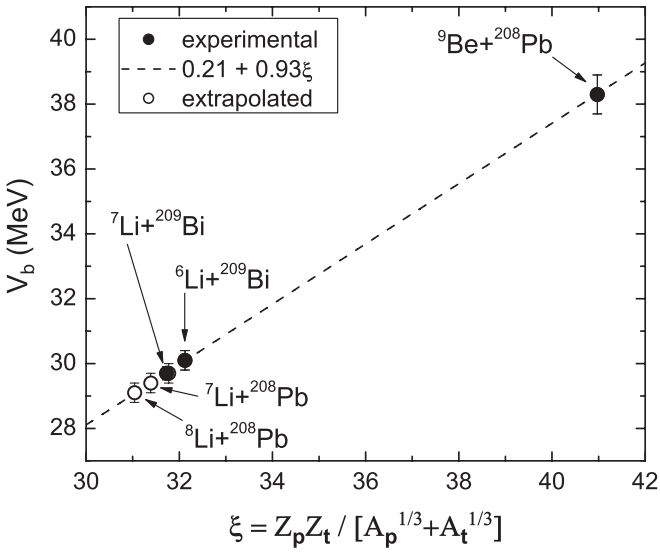

FIG. 4. Extrapolated barriers for ^{7,8}Li + ^{208}Pb. The experimental barriers for ^{6,7}Li + ^{209}Bi and ^{9}Be + ^{208}Pb are from Refs. [14,15], respectively.

experimentally determined [14,15]. A simple scaling with Z and A was used in the extrapolation procedure, as illustrated in Fig. 4. One would expect that the fusion barrier would vary linearly with $\xi = Z_p Z_t/[A_p^{1/3} + A_t^{1/3}]$ within a reduced range of Z's and A's so that ξ can be used to extrapolate. The three experimental points in the figure corroborate this expectation. In addition, ξ has been successfully used to scale energies when cross sections for different systems should be compared, as we will do in Sec. V (see also Ref. [4]). Once the barrier height was determined, an appropriate nuclear Woods-Saxon well and Coulomb potential were used to determine the corresponding radius and curvature parameters [44,45], with the results $V_b = 29.1$ MeV, $R_b = 11.5$ fm, $\hbar\omega = 4.4$ MeV. These can be compared with the Bass-barrier parameters $V_b = 29.7$ MeV, $R_b = 11.2$ fm, and $\hbar\omega = 4.4$ MeV. The dotted line in Fig. 3 represents the results of the BPM calculations while the dashed curves are the corresponding PACE2 results. More detailed coupled-channels calculations are not necessary for the present purposes because they should essentially coincide with the BPM results in the above-barrier regime [16]. It can be seen that the PACE2 calculations consistently overpredict the data. The solid curves in this figure show the result of multiplying the dashed curves by a factor of 0.7.

The experimental results for the two highest energies, where the two dominant evaporation residues were measured, can be used to determine the experimental fusion suppression factor SF_{exp}. The respective ratios of the total experimental cross section to that predicted by the BPM give an average value of 0.70 ± 0.02, which is our best estimation for SF_{exp}. This is consistent with the factor needed in Fig. 3 to bring the PACE2 predictions closer to the data for individual channels. A 6% systematic error must be assigned to SF_{exp}, related to a 0.3 MeV uncertainty in the barrier height. According to the statistical model, for $E_{c.m.} = 36.6$ and 37.5 MeV the missing cross section due to undetected residues amounts to less than 3% (see Table I). This value falls well within the reported systematic error. We emphasize that the above determination of SF_{exp} is based on comparison of purely experimental data with theory. To the extent that fusion suppression factors seem to be nearly energy independent [16], this determination using two points is justified. In the next two sections a model will be discussed that will allow us to obtain a suppression factor consistent with SF_{exp}, but determined for the whole energy region of the experiment.

IV. DISCUSSION OF ICF PROCESSES: MODEL CALCULATIONS

As noted above, a considerable suppression of the data with respect to BPM predictions is observed in Fig. 3. This suggests the possible presence of ICF processes if the fusion hindrance results from projectile breakup. In addition, statistical-model calculations using the code PACE2 do not reproduce the shape of the excitation function for ^{212}At if only CF is assumed. The predicted cross section after accounting for 30% suppression (0.7× PACE, solid curve) falls considerably below the data at the highest energy, and the experimental excitation function differs from the bell-shaped curve that is typical of neutron-evaporation yields from CF. In contrast, the ^{211}At data points are overpredicted by the same PACE2 calculation.

ICF has been explained as a two-step process where the projectile first breaks up and then one of the residual clusters fuses with the target. The cluster structure of ^{8}Li is primarily formed by a component of the type $(\alpha t)n$ [46]. Therefore, provided that breakup occurs, ICF processes involving fusion with clusters of ^{7}Li, α or $t(=^{3}\mathrm{H})$ might be expected, with probabilities that will depend on the energy of the particular cluster relative to the respective barrier. For cluster energies below the corresponding barrier, a negligible contribution from the ICF process might be expected, especially if it has to compete with ICF involving other clusters with above-barrier energies. These ideas can be used to provide further insight into the fusion processes that may be acting in the present system. Under the assumption that just after breakup but prior to ICF the clusters share the same velocity but together have a total kinetic energy diminished by the corresponding breakup (bu) energy, the available energy for fusion corresponding to each cluster may be estimated from the formula:

$$E^{x}_{\mathrm{c.m.}} = \frac{m_x(m_p + m_t)}{m_p(m_x + m_t)}\left(E^{p}_{\mathrm{c.m.}} - S_x\right), \qquad (1)$$

where $x = {}^{7}\mathrm{Li}, \alpha, t$; the index $p(t)$ refers to projectile (target), respectively, S_x is the threshold breakup energy for producing cluster x, and $E^{y}_{\mathrm{c.m.}}$ refers to the center of momentum of the y-target nuclei ($y = x$, p).

According to this formula, the clusters ^{7}Li, α, t possibly resulting from ^{8}Li breakup in the present experiment would have most probable center-of-momentum energies in the regions (26.4–31.2), (14.1–16.8), and (10.6–12.7) MeV, respectively. The corresponding fusion barriers are estimated to be 29.4 ± 0.6, 19.8 ± 0.7, and 10.0 ± 0.6 MeV (see Fig. 4 and Refs. [45,47]). It is therefore quite unlikely to have ICF with an α cluster in the present energy region, but ICF with t is very likely over the entire energy range of the present

experiment provided that breakup occurs. This ICF process would lead to the compound nucleus ^{211}Bi, which according to PACE2 decays $\sim 100\%$ of the time to ^{209}Bi through the $2n$ evaporation channel. Because this is an α-stable nucleus, our technique is "blind" to this process.

The ^{7}Li cluster, however, might start contributing to ICF in the upper half of the experimental energy region. This process would lead mainly to a ^{212}At residue after $3n$ evaporation, with a small amount of $4n$ decay to ^{211}At. Therefore, any contribution from this mechanism would be contained within the measured data and this might account for the unconventional shape of the measured excitation function for ^{212}At. To see how this process could affect the interpretation of the data, some model calculations accounting for this ICF mechanism were performed using PACE2. Two separate calculations were done for each bombarding energy, one for fusion of ^{8}Li and the other for fusion of ^{7}Li, where the ^{7}Li energy was calculated from the ^{8}Li energy by means of Eq. (1). The total fusion yields (for ^{8}Li and for ^{7}Li) were manually entered into PACE2 and the corresponding ^{211,212}At yields were determined. One condition of the model is that the sum of the ^{212}At yields from both PACE2 calculations should reproduce the corresponding experimental values. The other condition is exactly the same but for the ^{211}At yield. The input fusion cross sections were varied until the two conditions were simultaneously satisfied. In this way, the relative contribution of CF and ICF (with ^{7}Li) at each bombarding energy was determined from the best fit to the experimental data.

A possible concern in these model calculations is related to the fact that breakup is presumably a rather peripheral process and should affect mainly high partial waves. ICF would then occur with some angular momentum (L) selectivity, which may in turn affect the relative cross sections for the different evaporation residues [17,48,49]. Test calculations with PACE2 were conducted in which different L windows were introduced for the fusion of ^{7}Li + ^{208}Pb at the energies of interest. An L window was defined by excluding all partial waves below a given $L_{\min}$. Even for an $L_{\min}$ of one unit below the respective grazing value, the predicted ^{211,212}At fractional yields remained essentially constant. A maximum variation of 3% was estimated with respect to the calculation with no window, corresponding to the highest-energy case [$E_{\text{c.m.}}(^{7}\text{Li}) = 31.2$ or $E_{\text{c.m.}}(^{8}\text{Li}) = 37.5$ MeV]. The above effect safely can then be neglected, so no L window was used in the final calculations. The results are shown in Fig. 5, where the CF and ICF contributions are indicated. The threshold barrier for ICF with ^{7}Li falls at 35 MeV in the ^{8}Li energy scale. This is consistent with the best fit from the model, which indicates that this ICF process would have an increasingly large effect above this energy, especially on the ^{212}At yield.

One concern here is the fact that the evaporation residues are close to or on a closed shell. This could have substantial effects on the relative yields of the residues, which could possibly not be well accounted for in PACE2. One might expect that the main effects of closed shells would be related to corresponding changes in the phase space available for the residues, and that such effects would fade out with increasing excitation energy. We did some estimation of uncertainties for PACE2 calculations (see Table I) by varying the level-density parameter a between

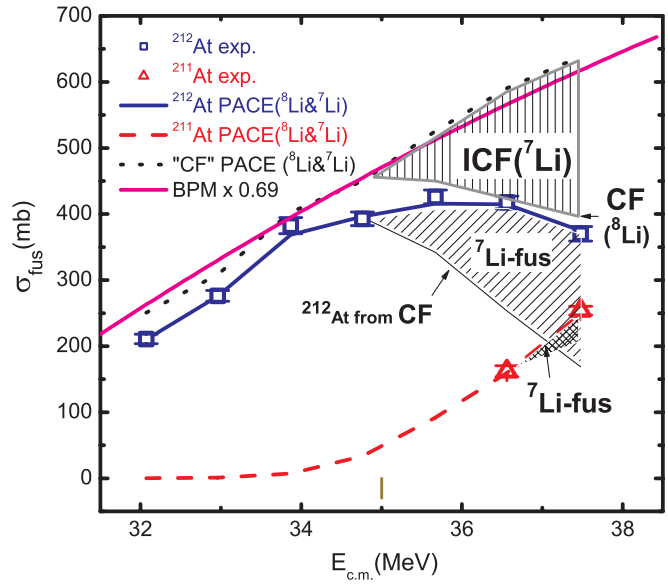

FIG. 5. (Color online) Model calculations to disentangle CF from ICF ($^{8}\text{Li} \rightarrow {}^{7}\text{Li} + n \rightarrow {}^{7}\text{Li}$ fusion + n). Both processes are included in the operational definition of complete fusion, "CF."

$a = A/7$ and $a = A/8$ (the default value used in PACE2 is $A/7.5$). This would account for some change in the available phase space. The fact that the relative yield of ^{212}At with respect to the total BPM prediction is well described by PACE2 at the four lowest energies, where shell effects are expected to be stronger for this channel, may be taken as an indication that shell effects, if any, are weak here. However, a possible effect of closed shells at the higher energies where the ^{211}At evaporation channel opens up cannot be discarded *a priori* and thus the above model calculations should be taken with due reserve. They are meant to show how the possibility of breakup prior to fusion followed by capture of the ^{7}Li fragment could affect the interpretation of the data.

V. ADOPTED CF CROSS SECTIONS AND COMPARISON WITH OTHER DATA

Because ^{7}Li has the same charge as ^{8}Li, both CF and ICF processes are included in an "operational" or "experimental" definition of complete fusion [14–16] that we denote as "CF." The resulting "CF" cross sections are reported in Table I, which in addition includes contributions from other, weaker evaporation channels predicted by PACE2 (column 4). The most important of these weaker channels is the one corresponding to $\alpha 3n$ evaporation, leading to the ^{209}Bi residue that cannot be detected in our experiment. Note that the values in the "CF" column actually are the result of a model fit, so they do not necessarily coincide exactly with the sum of columns 2–4. However, the difference is within the reported error bars. The values for the complete fusion cross sections that are adopted in the present work are those given in column "CF." Figure 5 illustrates that the "CF" cross sections are consistent with a suppression factor of about 0.69 with respect to the BPM predictions. The uncertainties in this "model" result can be expressed as $\text{SF}_{\text{mod}} = 0.69^{+.02}_{-.03}$. This is in good agreement with

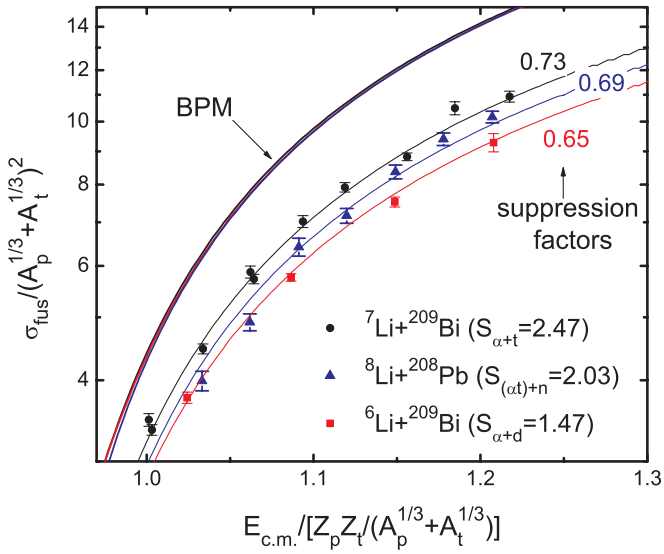

FIG. 6. (Color online) Reduced complete fusion cross sections ("CF") from the present work compared with data from Ref. [15]. The threshold breakup energies S_x are indicated (in MeV) for each projectile.

the experimental value reported in Sec. III, $SF_{exp} = 0.70 \pm 0.02$. Notice that SF_{mod} is actually energy independent, a result that can be obtained only if the experimental definition of "CF" is adopted.

To compare the present results with those reported for other Li isotopes [15], the data were scaled by dividing the experimental cross sections by the factor $(A_p{}^{1/3} + A_t{}^{1/3})^2$ and the energies by the factor $Z_pZ_t/(A_p^{1/3} + A_t^{1/3})$ (see Ref. [50]). The results are presented in Fig. 6. The BPM predictions for each system fall on top of each other in this plot, a consequence of the approximate proportionallity between corresponding barriers that is observed in Fig. 4. The effect of possible systematic errors in SF due to uncertainties in the barrier determination would be the same for the three systems as long as such a linear correlation between barriers holds. One way to look at this is by using the classical formula, which should nearly match the BPM in the region above the fusion barrier, $\sigma_{fus}/(\pi R^2) = 1 - V_b/E_{c.m.}$. If we call η the reduced energy defined in Fig. 6, then $E_{c.m.} = \eta\xi$. For $V_b \sim k\xi$, with k being some constant, the right-hand side of the above classical formula can be written as $1 - k/\eta$, an expression that no longer depends on the particular system. So our extrapolation procedure for the fusion barrier does actually allow us to directly compare the data for the three Li systems in the reduced plot of Fig. 6, thus effectively eliminating the possible effects of corresponding systematic errors in SF. The fact that the points of the present work fall in between those for ^{6}Li and ^{7}Li is in accordance with the observed correlation between suppression factors and the threshold breakup energies when heavy targets are used [15,16]. A reported suppression factor of 0.66 for ^{6}Li + ^{208}Pb [18] also is consistent with this conclusion within experimental uncertainties.

It has been pointed out that the effect of breakup on fusion is extremely complex to elucidate from a theoretical point of view [16,26,32,51]. Realistic models should incorporate variables such as the nuclear structure of the projectile and target, the various excitation mechanisms, and three-body tunneling among others. It is surprising that, in spite of this, a rather simple correlation seems to hold not only for different projectiles on the same target [19] but also for several Li isotopes on similar-A targets. The additional neutron-transfer modes present for ^{8}Li as compared to ^{6,7}Li projectiles, do not seem to affect the above conclusion as long as the "operational" definition of complete fusion ("CF"), in which the total charge of the projectile is absorbed, is adopted.

VI. SUMMARY AND CONCLUSIONS

We have measured fusion-evaporation cross sections for channels corresponding to complete fusion ("CF") in the ^{8}Li + ^{208}Pb system, at seven energies above the Coulomb barrier. A comparison with BPM calculations shows a hindrance of the data, with a suppression factor of 0.70 ± 0.02 (stat.) ± 0.04 (syst.). This suppression factor refers to the operational definition of complete fusion, where the whole charge but not necessarily the whole mass of the projectile is absorbed. A consideration of possible ICF processes supports the hypothesis that fusion with a ^{7}Li cluster might be contributing to the data in the upper half of the measured energy region. A simple model based on this hypothesis gives a good description of the data and allows the possible contribution of this particular ICF process to be estimated. A possible important contribution of ICF with a ^{3}H cluster is suggested. The present technique would be "blind" to this process, which would not, however, be included in the operational definition of fusion because the entire charge of the projectile is not absorbed. A comparison with similar data for the stable isotopes ^{6,7}Li appears to confirm a correlation between the suppression factor and the threshold breakup energy of the projectile. To complement the present results, a direct measurement of the different ICF yields is necessary.

ACKNOWLEDGMENTS

This work has been partially supported by the CONACYT (México) and by the US NSF under Grant Nos. PHY06-52591 and PHY07-58110. E.F.A. acknowledges the warm hospitality of all personnel at the Notre Dame Nuclear Structure Laboratory.

[1] E. F. Aguilera, J. J. Kolata, F. M. Nunes, F. D. Becchetti, P. A. DeYoung, M. Goupell, V. Guimaraes, B. Hughey, M. Y. Lee, D. Lizcano, E. Martinez-Quiroz, A. Nowlin, T. W. O'Donnell, G. F. Peaslee, D. Peterson, P. Santi, and R. White-Stevens, Phys. Rev. Lett. **84**, 5058 (2000).

[2] E. F. Aguilera, J. J. Kolata, F. D. Becchetti, P. A. DeYoung, J. D. Hinnefeld, A. Horvath, L. O. Lamm, Hye-Young Lee, D. Lizcano, E. Martinez-Quiroz, P. Mohr, T. W. O'Donnell, D. A. Roberts, and G. Rogachev, Phys. Rev. C **63**, 061603(R) (2001).

[3] N. Keeley, R. Raabe, N. Alamanos, J. L. Sida, Prog. Part. Nucl. Phys. **59**, 579 (2007).
[4] E. F. Aguilera, E. Martinez-Quiroz, D. Lizcano, A. Gómez-Camacho, J. J. Kolata, L. O. Lamm, V. Guimarães, R. Lichtenthäler, O. Camargo, F. D. Becchetti, H. Jiang, P. A. DeYoung, P. J. Mears, and T. L. Belyaeva, Phys. Rev. C **79**, 021601(R) (2009).
[5] L. F. Canto, P. R. S. Gomes, R. Donangelo, M. S. Hussein, Phys. Rep. **424**, 1 (2006).
[6] C. H. Dasso, S. Landowne, and A. Winther, Nucl. Phys. **A405**, 381 (1983).
[7] H. Feshbach, *Theoretical Nuclear Physics: Nuclear Reactions* (John Wiley & Sons, New York, 1992).
[8] J. P. Bychowski, P. A. DeYoung, B. B. Hilldore, J. D. Hinnefeld, A. Vida, F. D. Becchetti, J. Lupton, T. W. O'Donnell, J. J. Kolata, G. Rogachev, and M. Hencheck, Phys. Lett. **B596**, 26 (2004).
[9] P. A. DeYoung, Patrick J. Mears, J. J. Kolata, E. F. Aguilera, F. D. Becchetti, Y. Chen, M. Cloughesy, H. Griffin, C. Guess, J. D. Hinnefeld, H. Jiang, Scott R. Jones, U. Khadka, D. Lizcano, E. Martinez-Quiroz, M. Ojaniega, G. F. Peaslee, A. Pena, J. Rieth, S. VanDenDriessche, and J. A. Zimmerman, Phys. Rev. C **71**, 051601(R) (2005).
[10] J. J. Kolata, H. Amro, F. D. Becchetti, J. A. Brown, P. A. DeYoung, M. Hencheck, J. D. Hinnefeld, G. F. Peaslee, A. L. Fritsch, C. Hall, U. Khadka, Patrick J. Mears, P. O'Rourke, D. Padilla, J. Rieth, Tabatha Spencer, and T. Williams, Phys. Rev. C **75**, 031302(R) (2007).
[11] A. Chatterjee, A. Navin, A. Shrivastava, S. Bhattacharyya, M. Rejmund, N. Keeley, V. Nanal, J. Nyberg, R. G. Pillay, K. Ramachandran, I. Stefan, D. Bazin, D. Beaumel, Y. Blumenfeld, G. de France, D. Gupta, M. Labiche, A. Lemasson, R. Lemmon, R. Raabe, J. A. Scarpaci, C. Simenel, and C. Timis, Phys. Rev. Lett. **101**, 032701 (2008).
[12] D. Pereira, C. P. Silva, J. Lubian, E. S. Rossi, Jr., and L. C. Chamon, Phys. Rev. C **73**, 014601 (2006).
[13] L. F. Canto *et al.*, J. Phys. G: Nucl. Part. Phys. **36**, 015109 (2009).
[14] M. Dasgupta, D. J. Hinde, R. D. Butt, R. M. Anjos, A. C. Berriman, N. Carlin, P. R. S. Gomes, C. R. Morton, J. O. Newton, A. Szanto de Toledo, and K. Hagino, Phys. Rev. Lett. **82**, 1395 (1999).
[15] M. Dasgupta, D. J. Hinde, K. Hagino, S. B. Moraes, P. R. S. Gomes, R. M. Anjos, R. D. Butt, A. C. Berriman, N. Carlin, C. R. Morton, J. O. Newton, and A. Szanto de Toledo, Phys. Rev. C **66**, 041602(R) (2002).
[16] M. Dasgupta, P. R. S. Gomes, D. J. Hinde, S. B. Moraes, R. M. Anjos, A. C. Berriman, R. D. Butt, N. Carlin, J. Lubian, C. R. Morton, J. O. Newton, and A. Szanto de Toledo, Phys. Rev. C **70**, 024606 (2004).
[17] V. Tripathi, A. Navin, K. Mahata, K. Ramachandran, A. Chatterjee, and S. Kailas, Phys. Rev. Lett. **88**, 172701 (2002).
[18] Y. W. Wu, Z. H. Liu, C. J. Lin, H. Q. Zhang, M. Ruan, F. Yang, Z. C. Li, M. Trotta, K. Hagino, Phys. Rev. C **68**, 044605 (2003).
[19] A. Mukherjee, Subinit Roy, M. K. Pradhan, M. Saha Sarkar, P. Basu, B. Dasmahapatra, T. Bhattacharya, S. K. Basu, A. Chatterjee, V. Tripathi, and S. Kailas, Phys. Lett. **B636**, 91 (2006).
[20] L. R. Gasques, D. J. Hinde, M. Dasgupta, A. Mukherjee, and R. G. Thomas, Phys. Rev. C **79**, 034605 (2009).
[21] P. R. S. Gomes, I. Padron, E. Crema, O. A. Capurro, J. O. Fernández Niello, G. V. Marti, A. Arazi, M. Trotta, J. Lubian, M. E. Ortega, A. J. Pacheco, M. D. Rodríguez, J. E. Testoni, R. M. Anjos, L. C. Chamon, M. Dasgupta, D. J. Hinde, and K. Hagino, Phys. Lett. **B634**, 356 (2006).
[22] A. M. M. Maciel, P. R. S. Gomes, J. Lubian, R. M. Anjos, R. Cabezas, G. M. Santos, C. Muri, S. B. Moraes, R. L. Neto, N. Added, N. C. Filho, and C. Tenreiro, Phys. Rev. C **59**, 2103 (1999).
[23] K. Hagino, A. Vitturi, C. H. Dasso, and S. M. Lenzi, Phys. Rev. C **61**, 037602 (2000).
[24] C. Beck, F. A. Souza, N. Rowley, S. J. Sanders, N. Aissaoui, E. E. Alonso, P. Bednarczyk, N. Carlin, S. Courtin, A. Diaz-Torres, A. Dummer, F. Haas, A. Hachem, K. Hagino, F. Hoellinger, R. V. F. Janssens, N. Kintz, R. LiguoriNeto, E. Martin, M. M. Moura, M. G. Munhoz, P. Papka, M. Rousseau, A. SancheziZafra, O. Stezowski, A. A. Suaide, E. M. Szanto, A. Szanto de Toledo, S. Szilner, and J. Takahashi, Phys. Rev. C **67**, 054602 (2003).
[25] R. J. Woolliscroft, N. M. Clarke, B. R. Fulton, R. L. Cowin, M. Dasgupta, D. J. Hinde, C. R. Morton, and A. C. Berriman, Phys. Rev. C **68**, 014611 (2003).
[26] A. Diaz-Torres, I. J. Thompson, and C. Beck, Phys. Rev. C **68**, 044607 (2003).
[27] M. S. Hussein, L. F. Canto, and R. Donangelo, Nucl. Phys. **A722**, 321c (2003).
[28] A. Szanto de Toledo, F. A. Souza, C. Beck, S. J. Sanders, M. G. Munhoz, J. Takahashi, N. Carlin, A. A. P. Suaide, M. M. de Moura, and E. M. Szanto, Nucl. Phys. **A734**, 311 (2004).
[29] W. Y. So, S. W. Hong, B. T. Kim, and T. Udagawa, Phys. Rev. C **69**, 064606 (2004).
[30] P. R. S. Gomes, M. D. Rodriguez, G. V. Marti, I. Padron, L. C. Chamon, J. O. Fernandez Niello, O. A. Capurro, A. J. Pacheco, J. E. Testoni, A. Arazi, M. Ramirez, R. M. Anjos, J. Lubian, R. Veiga, R. Liguori Neto, E. Crema, N. Added, C. Tenreiro, and M. S. Hussein, Phys. Rev. C **71**, 034608 (2005).
[31] L. F. Canto, R. Donangelo, and H. D. Marta, Phys. Rev. C **73**, 034608 (2006).
[32] L. F. Canto, R. Donangelo, and M. S. Hussein, Nucl. Phys. **A787**, 243c (2007).
[33] C. J. Lin, H. Q. Zhang, F. Yang, M. Ruan, Z. H. Liu, Y. W. Wu, X. K. Wu, P. Zhou, C. L. Zhang, G. L. Zhang, G. P. An, H. M. Jia, and X. X. Xu, Nucl. Phys. **A787**, 281c (2007).
[34] J. J. Kolata, V. Z. Goldberg, L. O. Lamm, M. G. Marino, C. J. O'Keeffe, G. Rogachev, E. F. Aguilera, H. Garcia-Martinez, E. Martinez-Quiroz, P. Rosales, F. D. Becchetti, T. W. O'Donnell, D. A. Roberts, J. A. Brown, P. A. DeYoung, J. D. Hinnefeld, and S. A. Shaheen, Phys. Rev. C **65**, 054616 (2002).
[35] A. Gómez-Camacho and E. F. Aguilera, Nucl. Phys. **A735**, 425 (2004).
[36] A. M. Moro, R. Crespo, H. Garcia-Martinez, E. F. Aguilera, E. Martinez-Quiroz, J. Gómez-Camacho, and F. M. Nunes, Phys. Rev. C **68**, 034614 (2003).
[37] A. M. Moro, R. Crespo, H. García-Martínez, E. F. Aguilera, E. Martinez-Quiroz, J. Gómez-Camacho, and F. M. Nunes, Rev. Mex. Fís. **49**, S4, 73 (2003), http://rmf.fciencias.unam.mx/pdf/rmf-s/49/4/49_4_073.pdf.
[38] F. D. Becchetti, R. S. Raymond, D. A. Roberts, J. Lucido, P. A. DeYoung, B. Hilldore, J. Bychowski, A. J. Huisman, P. J. VanWylen, J. J. Kolata, G. Rogachev, and J. D. Hinnefeld, Phys. Rev. C **71**, 054610 (2005).

[39] E. F. Aguilera *et al.*, Rev. Mex. Fís. **50**, S2, 1 (2004), (http://rmf.fciencias.unam.mx/pdf/rmf-s/50/2/50_2_001.pdf); **53**, S6, 1 (2007), (http://rmf.fciencias.unam.mx/pdf/rmf-s/53/6/53_6_001.pdf).

[40] J. J. Kolata, V. Guimaraes, D. Peterson, P. Santi, R. White-Stevens, P. A. DeYoung, G. F. Peaslee, B. Hughey, B. Atalla, M. Kern, P. L. Jolivette, J. A. Zimmerman, M. Y. Lee, F. D. Becchetti, E. F. Aguilera, E. Martinez-Quiroz, and J. D. Hinnefeld, Phys. Rev. Lett. **81**, 4580 (1998).

[41] A. Gavron, Phys. Rev. C **21**, 230 (1980).

[42] For radioactive nuclei with decay constant λ that are being produced at some rate P, the respective activity A follows the well known decay law $dA/dt = \lambda(P - A)$. If only one cycle of the pulsed beam is considered, the solution can be given by two functions, one valid during the time (t_{on}) that the beam is on (A_1) and the other one valid afterwards (A_2): $A_1(t) = P(1 - e^{-\lambda t})$, $A_2(t) = A_1(t_{on})e^{-\lambda(t-t_{on})}$. The integral of $A_2(t)$ over any time interval can thus be easily related to P and therefore to the respective cross section. This method, with the additional assumption that each beam-on cycle contributes only to the counts in the two succesive beam-off periods, was used by one group (ININ) to deduce the cross sections for ^{212}At production. Alternatively, the periodic step function P corresponding to a whole experimental run can be used in the decay law and an exact numeric solution for A can be found. This method was used by the second group (Hope College). For the case of ^{211}At the procedure is somewhat simpler but the detailed history of the bombardement must be taken into account.

[43] R. Bass, Phys. Rev. Lett. **39**, 265 (1977).

[44] R. A. Broglia and A. Winther, *Heavy Ion Reactions* (Benjamin, Reading, MA, 1981), Vol. I.

[45] L. C. Vaz, J. M. Alexander, and G. R. Satchler, Phys. Rep. **69**, 373 (1981).

[46] Y. Suzuki, R. G. Lovas, K. Yabana, and K. Varga, *Structure and Reactions of Light Exotic Nuclei* (Taylor & Francis, London, 2003).

[47] R. K. Puri and R. K. Gupta, in *Proceedings of the International Conference on Heavy Ion Fusion: Exploring the Variety of Nuclear Properties, Padova, 1994*, edited by A. M. Stefanini, G. Nebbia, S. Lunardi, G. Montagnoli, and A. Vitturi (World Scientific, Singapore, 1994), p. 319.

[48] B. Haas *et al.*, Phys. Rev. Lett. **54**, 398 (1985).

[49] M. Dasgupta, A. Navin, Y. K. Agarwal, C. V. K. Baba, H. C. Jain, M. L. Jhingan, and A. Roy, Phys. Rev. Lett. **66**, 1414 (1991).

[50] P. R. S. Gomes, J. Lubian, I. Padron, and R. M. Anjos, Phys. Rev. C **71**, 017601 (2005).

[51] D. J. Hinde, M. Dasgupta, B. R. Fulton, C. R. Morton, R. J. Wooliscroft, A. C. Berriman, and K. Hagino, Phys. Rev. Lett. **89**, 272701 (2002).